



VCU

Virginia Commonwealth University
VCU Scholars Compass

Theses and Dissertations

Graduate School

2023

Poly(TFEMA) Surface Coating Applied on Perovskite Thin Films using Supercritical Carbon Dioxide.

Kasey Handy

Follow this and additional works at: <https://scholarscompass.vcu.edu/etd>

© The Author

Downloaded from

<https://scholarscompass.vcu.edu/etd/7406>

This Thesis is brought to you for free and open access by the Graduate School at VCU Scholars Compass. It has been accepted for inclusion in Theses and Dissertations by an authorized administrator of VCU Scholars Compass. For more information, please contact libcompass@vcu.edu.

**Poly(TFEMA) Surface Coating Applied on Perovskite Thin Films using
Supercritical Carbon Dioxide**

Kasey Handy

AS Computer Science, Northern Virginia Community College, 2021

BS Biomedical Engineering, Virginia Commonwealth University, 2021

Advisor: Dr. Gary Tepper

Interim Dean of College of Engineering

Virginia Commonwealth University

Richmond, Virginia

May, 2023.

Acknowledgements

Thank you for the support from all of VCU College of Engineering Department of Mechanical and Nuclear Engineering. Additionally the Nanometer Materials Core Characterization Facility at VCU for the help of the material characterization. Specifically I would like to thank my advisor Dr. Tepper for his guidance throughout the project.. I would also like to thank Dr. Mossi for introducing me to this opportunity in the program and helping me throughout the process. Thank you to all the faculty at the NCC, including Dr. Pestov, Dr. Bertino, and Dr. Mayer for teaching me so much and being a great help. Lastly, thank you Dr. Castano and Dr. Pestov for joining this committee.

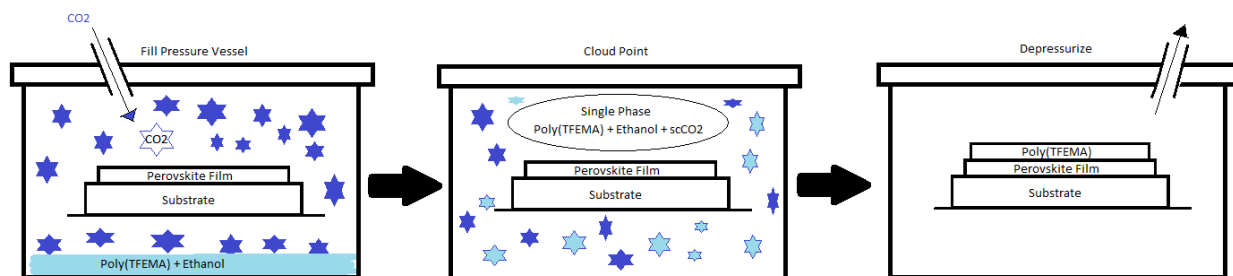
Table Of Contents:

	Page
Acknowledgements.....	2
List of figures.....	4
Abstract.....	5
Chapter	
1 Introduction	
1.1 History of Organic-Inorganic Halide Perovskite Solar Cells.....	5
1.2 Fabrication Methods of Perovskite Solar Cells.....	7
1.3 History of Supercritical CO ₂	8
1.4 Application of Supercritical CO ₂ for Perovskite Solar Cells.....	9
1.5 Effects of Supercritical CO ₂ and Cosolvents.....	10
1.6 History of Cosolvents Poly(TFEMA) & Ethanol.....	10
1.7 Thesis Objective.....	12
2 Experimental Methods	
2.1 Device Fabrication (Material and precursor preparation).....	12
2.2 SFT Setup and Procedure for Cloud Point Determination.....	13
2.3 Pressure Vessel Setup and Procedure for Deposition.....	14
2.4 Device Characterization.....	16
3 Results and Discussion	
3.1 Phase behaviors of Poly(TFEMA) & Ethanol in ScCO ₂	16
3.2 Raman Spectroscopy Results of Poly(TFEMA) surface coating.....	17
3.3 SEM Results of Poly(TFEMA) surface coating.....	18
4 Conclusion.....	19
References.....	21

List of Figures:

Figure 1. Perovskite Solar Cell.....	6
Figure 2. Chemical Structure of $\text{CH}_3\text{NH}_3\text{PbI}_3$	7
Figure 3. Thin film deposition by spin coating.....	8
Figure 4. Phase Diagram of Carbon Dioxide.....	9
Figure 5. Crystallization of $\text{CH}_3\text{NH}_3\text{PbI}_3$ perovskite films in supercritical carbon dioxide.....	10
Figure 6. Cloud-point curves of 0.3 and 1.0 wt% poly(TFEMA) solutions in scCO_2	11
Figure 7. SFT Phase Monitor Setup.....	14
Figure 8. Top view of SFT Pressure Vessel and Camera Setup.....	14
Figure 9. Pressure Vessel and Pump Setup.....	15
Figure 10. Dissolved solution at 1555 psi and 32°C	16
Figure 11. Cloud point of solution at 1100 psi and 31°C	17
Figure 12. Raman Spectroscopy Results.....	17
Figure 13. SEM of Perovskite Layer.....	18
Figure 14. SEM of Perovskite Layer with Poly(TFEMA) Deposition.....	19

Graphical Abstract:



Abstract:

Perovskite-based solar cells face challenges with stability due to external environment conditions; especially moisture. A new production to counteract this is reported.

Poly(trifluoroethyl methacrylate) is applied as a thin film to improve hydrophobicity of the CH₃NH₃PbI₃ films; this post deposition treatment is processed using supercritical carbon dioxide accompanied by ethanol. The quality of the Poly(TFEMA) deposition is analyzed using Raman Spectroscopy and Scanning Electron Microscopy.

1. Introduction

1.1 History of Organic-Inorganic Halide Perovskite Solar Cells

Perovskite solar cells offer a new renewable energy source capable of efficiently converting sunlight into electricity. They are cost-effective and have easy solution manufacturing. Organic-inorganic metal halide perovskite solar cells have achieved cell efficiencies exceeding 25% as of January 26, 2022 [1]. This is due to their excellent electronic and optical properties including high absorption [2], small exciton binding energy [3], high carrier mobility [4], large carrier diffusion length [5], bandgap tunability [6], and high tolerance for defects [7]. However, challenges of perovskite cells include exposure to external

environmental factors (temperature, humidity, radiation) that hinder long-term stability, fabrication (large scale production and high quality films/crystals), and toxicity of materials.

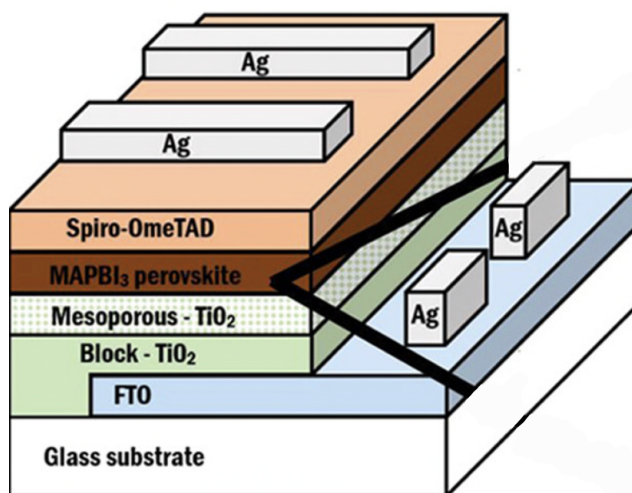


Figure 1. Perovskite Solar Cell [8]

Organic-inorganic hybrid perovskites ($\text{CH}_3\text{NH}_3\text{PbI}_3$) have an ABX_3 crystal structure composed of 3 ions: ion A is generally an organic cation such as an organic ammonium (e.g. methylammonium or formamidinium), ion B is typically an inorganic cation such as lead or tin, and ion X is typically a halide or oxide anion such as iodide, bromide, or chloride [9]. The ABX_3 is a three-dimensional network of BX_6 octahedral structure with the “A” ion filled in the octahedral void [10]. Materials with cubic lattice nested octahedral layered structures possess excellent photoelectric properties (high power conversion efficiency), lower exciton binding energy (high exciton splitting efficiency), high exciton diffusion enabled by long diffusion length, and high optical absorption coefficients (absorbed photons that are converted to electrons and collected at the electrodes) [11]. The material choices for each ion will be essential to

determining the optical and electronic properties. The objective is a perovskite that exhibits strong light absorption, long charge-carrier lengths, suitable band gap, and simple manufacturing.

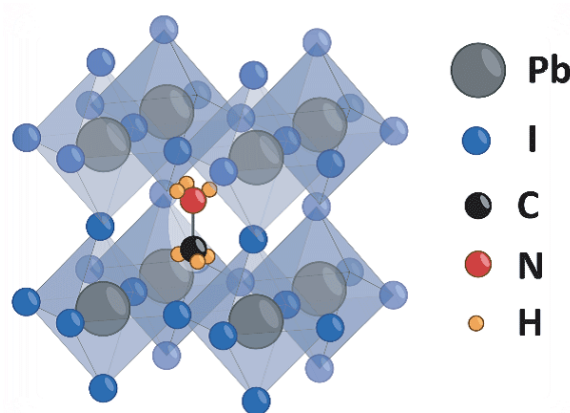


Figure 2. Chemical Structure of $\text{CH}_3\text{NH}_3\text{PbI}_3$ [12]

1.2 Fabrication Methods of Perovskite Solar Cells

In general, perovskite films are processed by either vacuum or solution methods. Common fabrication methods include one-step solution deposition, two-step solution-based processing, dual-source vapor deposition, sequential vapor deposition, and vapor-assisted solution processing. The one-step solution deposition method involves spin coating a solution containing organic and inorganic components on a substrate and then annealing to form perovskite. The two-step solution-based method is similar except there are two spin coating steps, the first solution being an inorganic component and the second an organic component followed by annealing. The dual-source vapor deposition method involves evaporating the organic and inorganic components and then annealing. The sequential vapor deposition method creates a bilayer film of the inorganic and organic components by preparing the sequential deposition, followed by thermal annealing. Lastly, the vapor assisted solution process starts with an

inorganic component spin-coated onto the substrate, which is then exposed to vapors of organic components at an elevated temperature [13]. The main concerns during fabrication of solar cells is film quality and thickness. From a manufacturing point of view, production at large scale is difficult using spin-coating. New technologies meant to be compatible with manufacturing include: roll-roll process, spray-coating, doctor-blade coating, soft-cover deposition, drop casting, ultrasonic coating, and electrospray. [14]

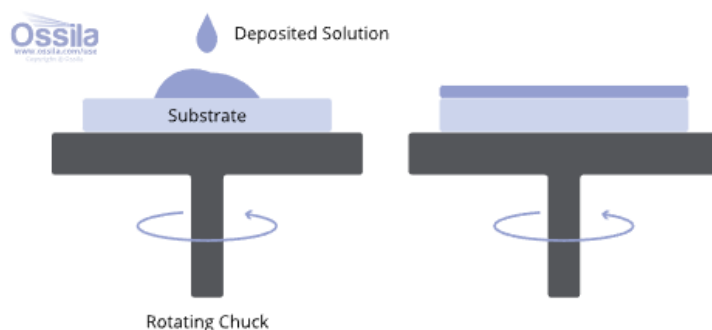


Figure 3. Thin film deposition by spin coating [15]

1.3 History of Supercritical CO₂

Supercritical fluids have existed for a number of years as a common method to synthesize nanostructured materials [16]. The phenomenon occurs when a material is brought above its critical point, creating a combination of gas and liquid-like properties (e.g density, viscosity, diffusion coefficient). Most commonly used in this approach is supercritical CO₂ fluid since it is non-toxic, non-flammable, non-reactive, inexpensive, environmentally friendly and energy efficient (moderate critical temperature and pressure). ScCO₂ has an easy to achieve cloud point with a temperature of 31.1 celsius and 73.8 bar. The thermophysical properties of CO₂ can be changed easily by adjusting the temperature and pressure of the environment. This allows

supercritical CO₂ to be used as either the solvent, anti-solvent, solute, or reaction medium during processing [17].

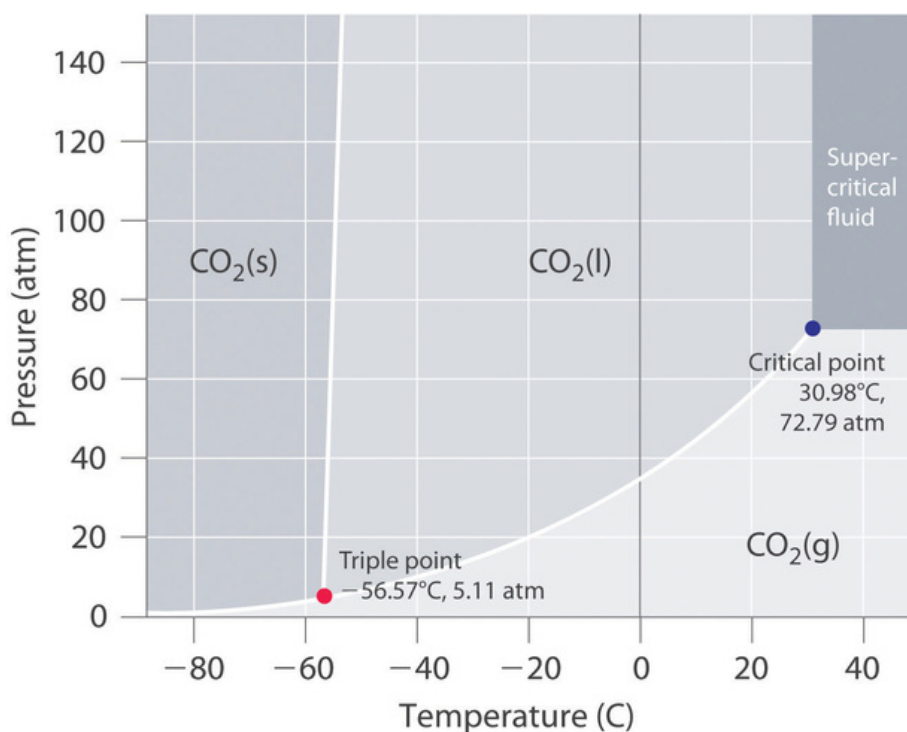


Figure 4. Phase Diagram of Carbon Dioxide [18]

1.4 Application of Supercritical CO₂ for Perovskite Solar Cells

Gilbert Annohene demonstrated a post-treatment annealing for perovskite solar cells in supercritical fluid CO₂[8]. The scCO₂ acts as an antisolvent during the solid-state film crystallization with the advantage that it does not leave any harmful solvent residuals. This is done by releasing the pressure allowing it to enter the gas phase without crossing a phase boundary. Results accelerates the solid-state kinetics increasing crystallinity and average grain size of CH₃NH₃PbI₃ films [8]. The combination of larger grains and enhanced crystalline

quality of grain can reduce the overall bulk defect density and mitigate hysteresis by suppressing charge trapping during solar cell operation [19].

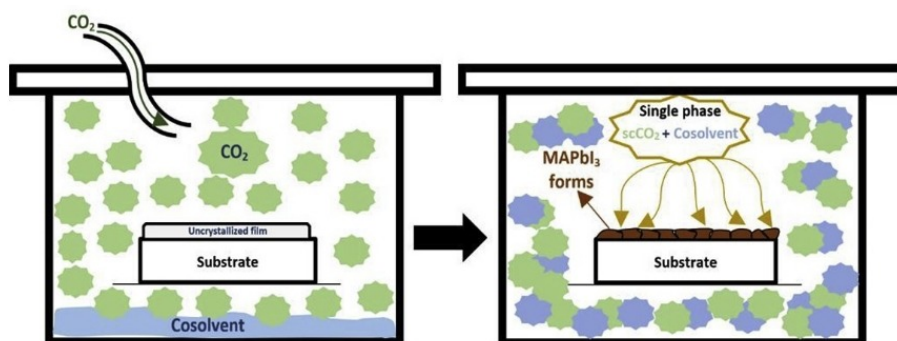


Figure 5. Crystallization of CH₃NH₃PbI₃ perovskite films in supercritical carbon dioxide [20]

1.5 Effects of Supercritical CO₂ and Cosolvents

Here, the use of solely supercritical CO₂ fluid will be extended to include the addition of an organic cosolvents and fluoropolymer to the scCO₂ for a post deposition film. Both the Ethanol and Poly(TFEMA) are completely soluble in supercritical CO₂ [21, 22] at the concentrations used allowing for a binary single-phase supercritical fluid. When above cloud point, the solution can be depressurized slowly allowing for the precipitation of Poly(TFEMA) onto the sample of perovskite, forming a thin layer.

1.6 History of Cosolvents Poly(TFEMA) & Ethanol

Poly(TFEMA) is a fluorinated polymer known to have excellent heat and chemical resistance, low refractive index, weatherability, non-cohesiveness, water and oil repellency, transparency, and electric insulating properties; these characteristics allow it to be used in various coating applications [22, 23]. The polymer can be easily produced by free radical polymerization

using bulk, solution, and emulsion polymerization methods with supercritical carbon dioxide as the polymerization medium [23, 24]. Figure 5 displays the results from Ratcharak and Sane on the cloud point of Poly(TFEMA) in supercritical CO₂ with weight percentages of 0.3-1.0% [25].

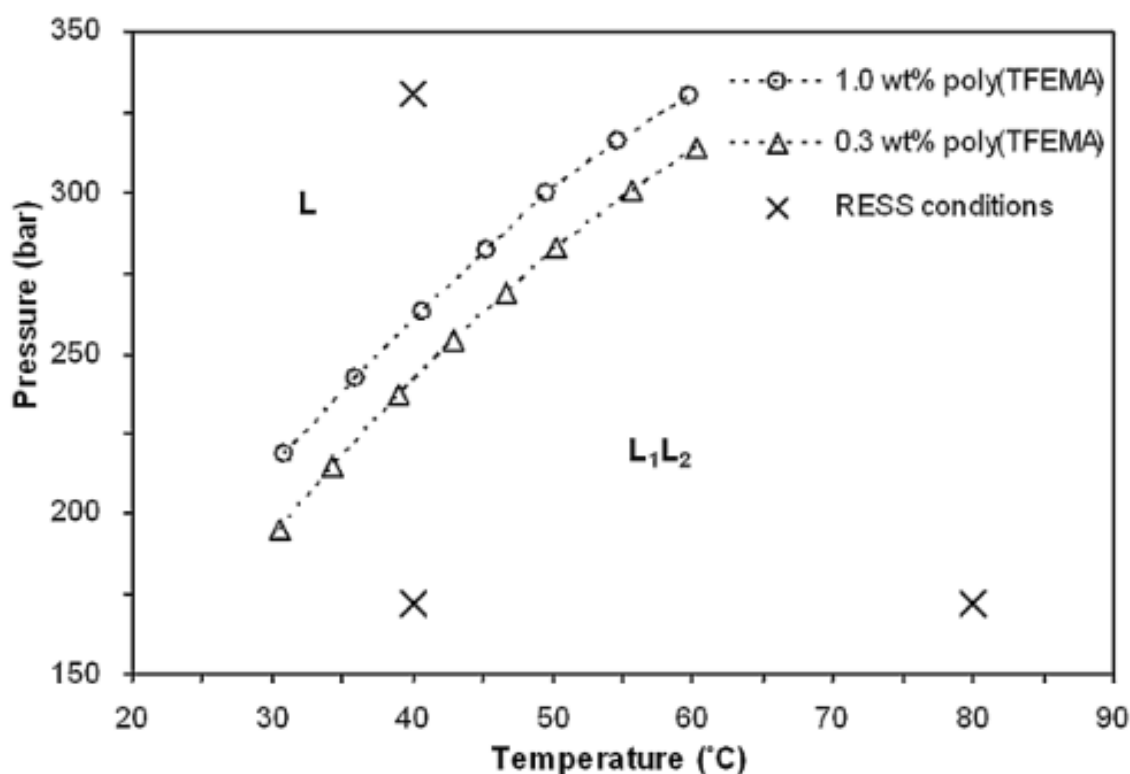


Figure 6. Cloud-point curves of 0.3 and 1.0 wt% poly(TFEMA) solutions in supercritical CO₂ [25]

Ethanol is added to the solution to decrease cloud point [26]. The lower cloud point allows for the experiment to be conducted in a standard pressure vessel, compared to using more expensive, higher pressure equipment. The ethanol as an organic cosolvent in supercritical carbon dioxide may also have an effect on the crystallization of the CH₃NH₃PbI₃ film, causing variations in grain size and general film morphology [20].

1.7 Thesis Objective

The objective of this experiment is to create a coating of Poly(TFEMA) onto Perovskite thin films in Supercritical Carbon Dioxide. Cloud point determination of solution containing Poly(TFEMA), Ethanol, and scCO₂ was determined experimentally using Supercritical Fluid Technologies, Inc. (SFT) Phase Monitor I Generation. Raman Spectroscopy and Horiba Scientific LabSpec 6 software was used to characterize the chemical structure of the Perovskite film before and after deposition onto the film. Surface coverage is obtained from Scanning Electron Microscope (SEM) (Hitachi SU-70 FE-SEM) and ImageJ software.

2. Experimental Methods

2.1 Device Fabrication (Material and precursor preparation)

Devices were prepared on 25 mm by 25 mm fluorine-doped tin oxide (FTO) glass substrates (Ossila, TEC 15). Substrate cleaning included; washing with detergent and deionized water, ultrasonic bath in 2% Hellmanex solution, rinsing with deionized water, ultrasonic bath in isopropanol for 15 minutes, ultrasonic bath in acetone for 15 minutes, rinsing with acetone, rinsing with isopropanol, drying the isopropanol with dry air, and plasma cleaning for 4 minutes.

Perovskite layer ($\text{CH}_3\text{NH}_3\text{PbI}_3$) was synthesized by 1:1:1 molar ratio of: 2.385 g methyl ammonium iodide ($\text{CH}_3\text{NH}_3\text{I}$) (98%, Sigma-Aldrich), 6.915 g lead (II) iodide (PbI_2) (99.9985%, Alfa Aesar), and 1.063 mL dimethyl sulfoxide (DMSO) (>99.9%, anhydrous, Sigma-Aldrich), then put in 9.484 mL N,N-dimethylformamide (DMF) (>99.8%, anhydrous, Sigma-Aldrich) and 0.3 mL diethyl ether (>99.8%, anhydrous, Sigma-Aldrich). The solution was stirred for one hour at room temperature and filtered using a 0.2 μm syringe filter (Corning Inc.). The solution was then spin-coated onto substrate at 6000 rpm for 25 sec and 0.6 mL diethyl ether

was dripped onto the rotating surface 6 sec into spinning. Spin coating was done in an argon-filled glove box. Substrates were then placed on a hot plate at 50°C for 30 min.

2.2 SFT Setup and Procedure for Cloud Point Determination

The determination of cloud point for the mixture of 0.02 weight percent ethanol, 0.03 weight percent Poly(TFEMA) and 0.95 weight percent of scCO₂ was found utilizing the Supercritical Fluid Technologies, Inc. (SFT) Phase Monitor I Generation 1. 3.54 grams of Poly(TFEMA) and 3 mL of Ethanol were loaded into the SFT-Phase monitor 30cc processing vessel. The light control dial was adjusted until the sample could be properly viewed through a quartz window. This image was captured using a CCD camera in front of Quartz window connected to a monitor. The cell was slowly filled with carbon dioxide with a helium headspace and siphon tank (Airgas), then heated to 31°C using variable transducers and flexible heating cords wrapped around the cylinder. Once the temperature reached 31°C, the wheel was turned clockwise till pressure reached approximately 1500 psi. After pressure was met and solution was visibly completely dissolved, the wheel was turned counterclockwise to depressurize. Oscillating the wheel between 12,500 and 900 psi showed the transitions of the cloud point.



Figure 7. SFT Phase Monitor Setup

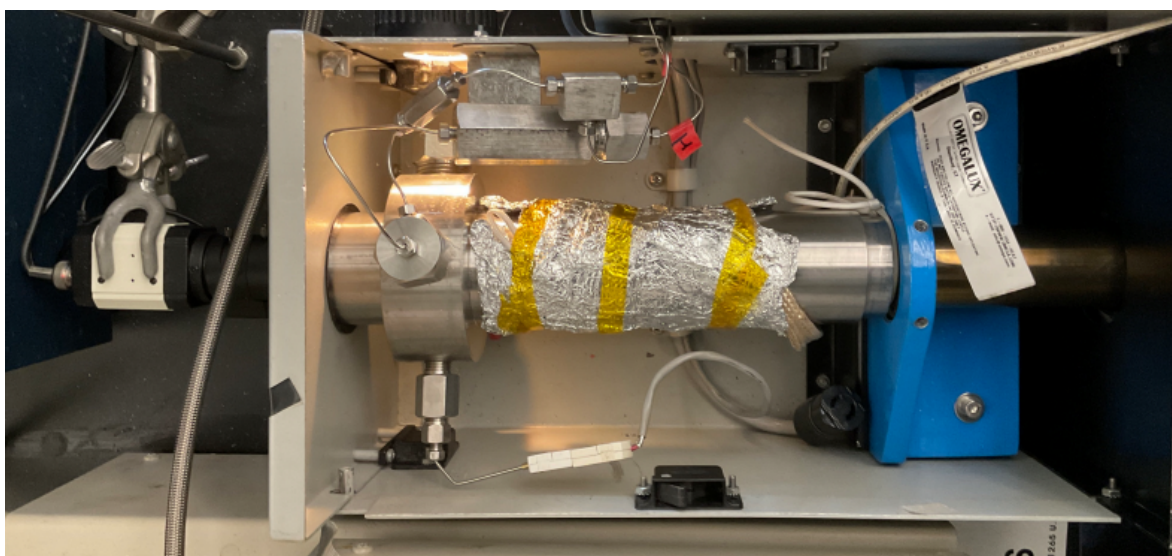


Figure 8. Top view of SFT Pressure Vessel and Camera Setup

2.3 Pressure Vessel Setup and Procedure for Deposition

After the completed fabrication process, the substrates were placed into a 600mL pressure vessel (Parr instrument Pressure Reactor 4768). A mixture of 0.02 weight percent

ethanol and 0.03 weight percent Poly(TFEMA) and 0.95 weight percent of scCO₂ was used during the deposit. 7.086 grams of Poly(TFEMA) and 6 mL of Ethanol were loaded into the bottom of the pressure vessel. A syringe pump (Teledyne ISCO Pump 260D) was used to pressurize the CO₂, Ethanol, Poly(TFEMA) mixture for the Poly(TFEMA) deposition. The experiment was carried out at the same temperature (31°C) and pressure (1000 psi) for the cloud point found in the SFT phase monitor. This pressure and temperature was held for 10 minutes and then depressurized slowly for another 10 minutes. The slow depressurization allows for the Poly(TFEMA) to come out of cloud point allowing it to precipitate onto the perovskite film. This led to a deposition of Poly(TFEMA) on top of the perovskite film.

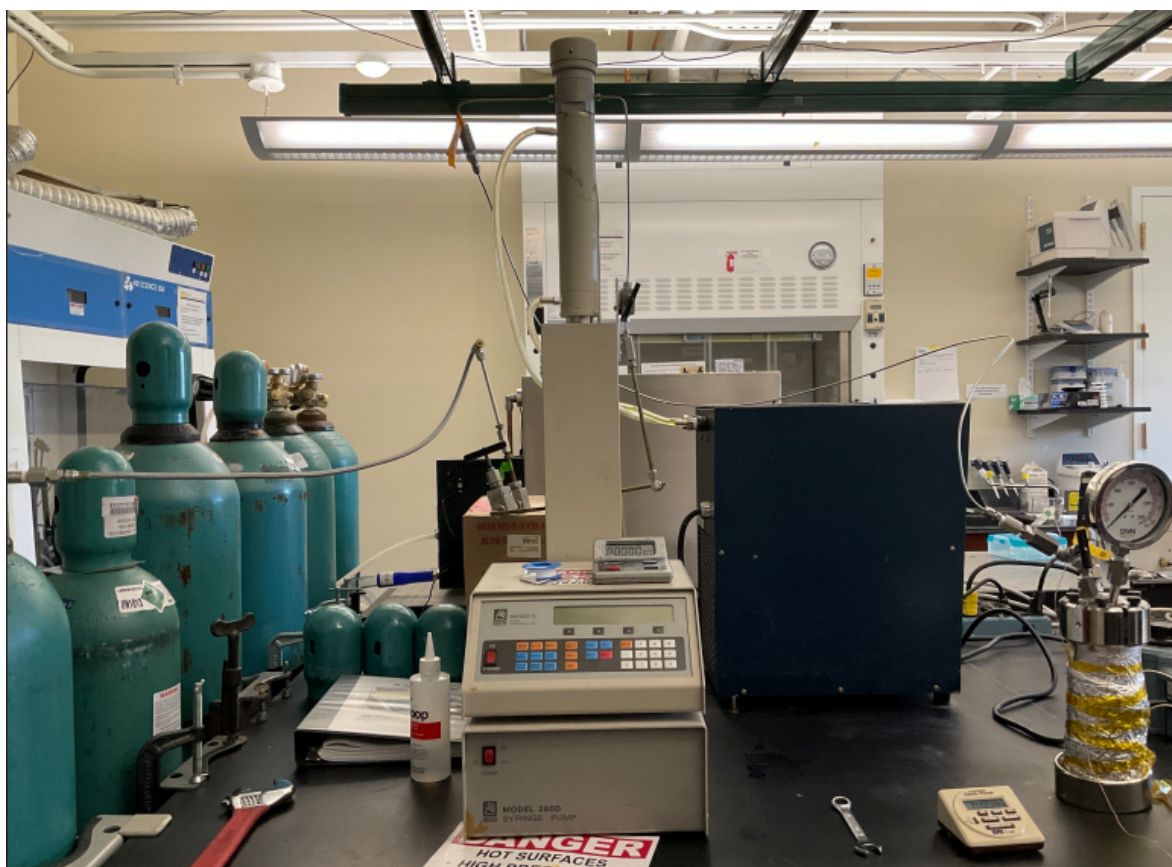


Figure 9. Pressure Vessel and Pump Setup

2.4 Device Characterization

Raman spectroscopy with Horiba Scientific LabSpec 6 software was used to characterize the chemical structure of the perovskite film and deposition of Poly(TFEMA). Scanning Electron Microscope (SEM) (Hitachi SU-70 FE-SEM) at 20 kV and ImageJ software is used to characterize the substrate's surface.

3. Results and Discussion

3.1 Phase behaviors of Poly(TFEMA) & Ethanol in scCO_2

Cloud-point pressures of 0.03 poly(TFEMA) and 0.02 wt% Ethanol solutions in supercritical carbon dioxide were found at a pressure of ~ 1100 to ~ 900 psi and a temperature of 31°C . Figure 1 displays the soluble and completely dissolved poly(TFEMA) and Ethanol in scCO_2 . Precipitation of solution begins at approximately 1100 psi during depressurization. A visible white cloud appears in Figure 2 illustrating a fully precipitated and non-soluble Poly(TFEMA) and Ethanol in scCO_2 .



Figure 10. Dissolved solution at 1555 psi and 32°C

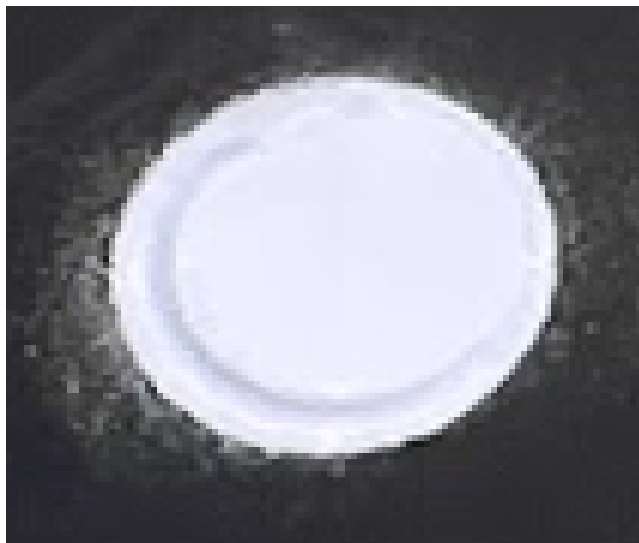


Figure 11. Cloud point of solution at 1100 psi and 31°C

3.2 Raman Spectroscopy Results of Poly(TFEMA) surface coating

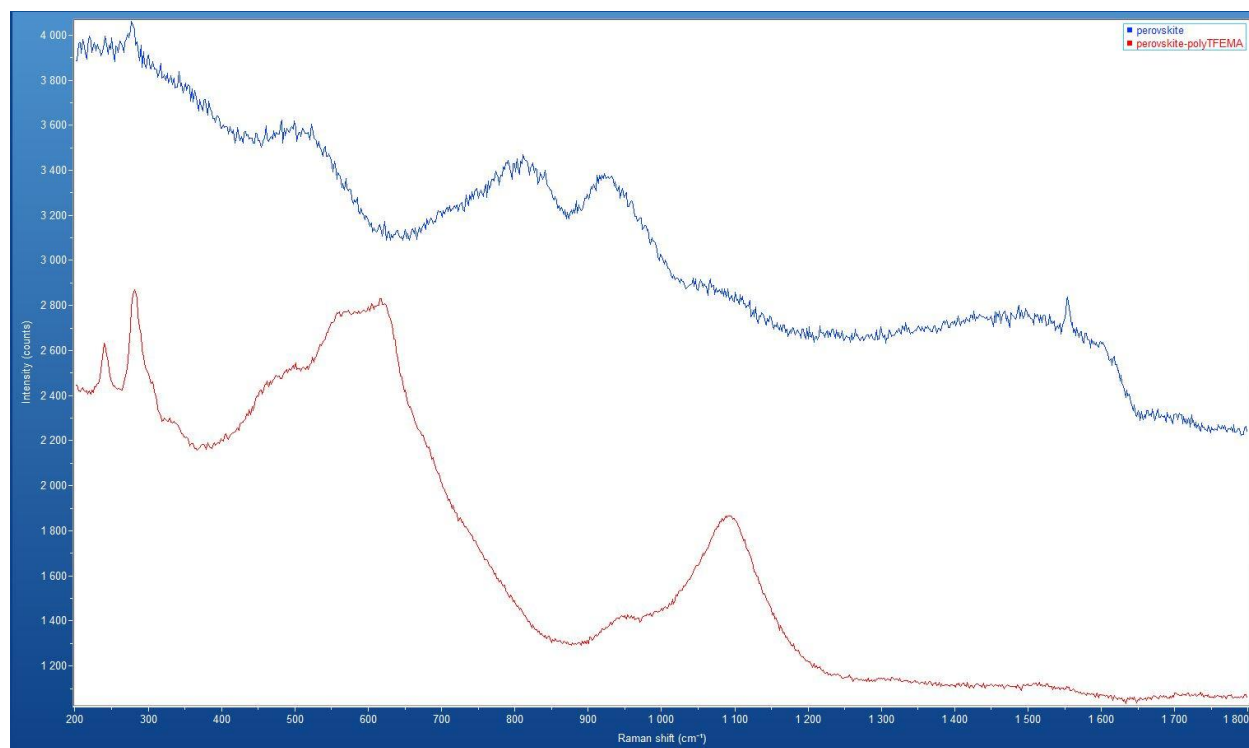


Figure 12. Raman Spectroscopy Results

Raman Spectroscopy was performed to characterize the sample film's composition variation before and after the deposition of Poly(TFEMA). Figure 10 shows the Raman spectrums measured at an excitation wavelength of 532 nm. The blue line represents a perovskite film without any deposit of fluoropolymer and the red line represents the perovskite film that did undergo the deposition of fluoropolymer in supercritical CO₂. Comparison between the two results shows a clear distinction between the two samples that confirms the deposition of Poly(TFEMA). Peak positions of the sole Perovskite include 275 (cm⁻¹), 500 (cm⁻¹), 850 (cm⁻¹) and 950 (cm⁻¹). Compared to the Perovskite with the fluoropolymer deposit, its peak positions include 225 (cm⁻¹), 275 (cm⁻¹), 600 (cm⁻¹), and 1100 (cm⁻¹). It is assumed that the Poly(TFEMA) deposit is a result of the peak at 600 (cm⁻¹) and 1100 (cm⁻¹)

3.3 SEM Results of Poly(TFEMA) surface coating

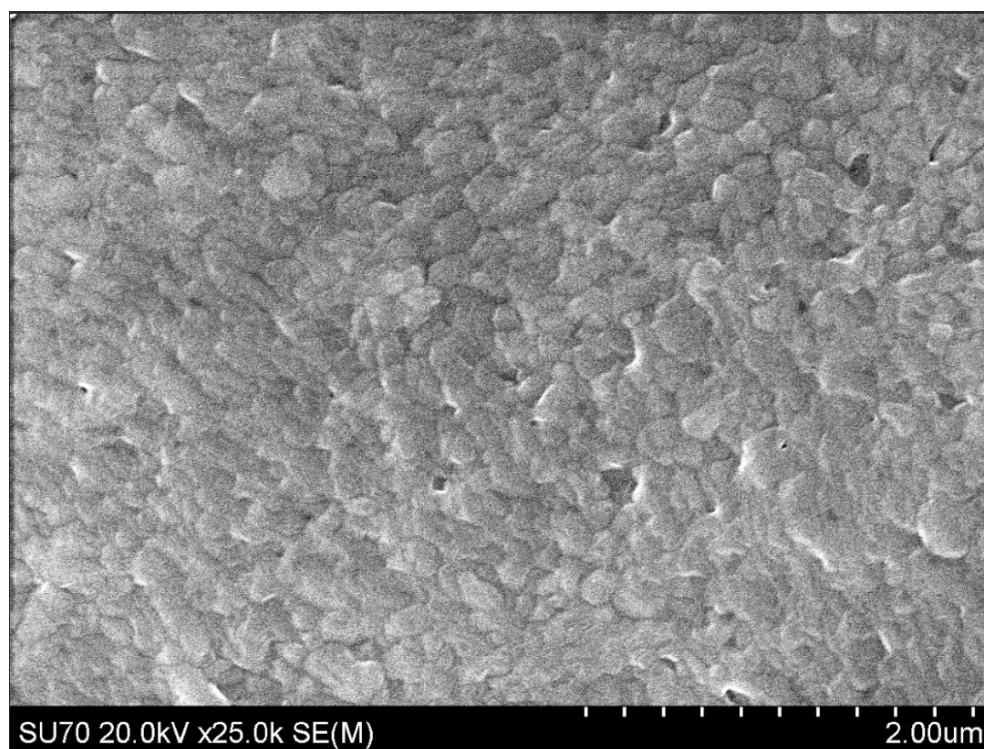


Figure 13. SEM of Perovskite Layer

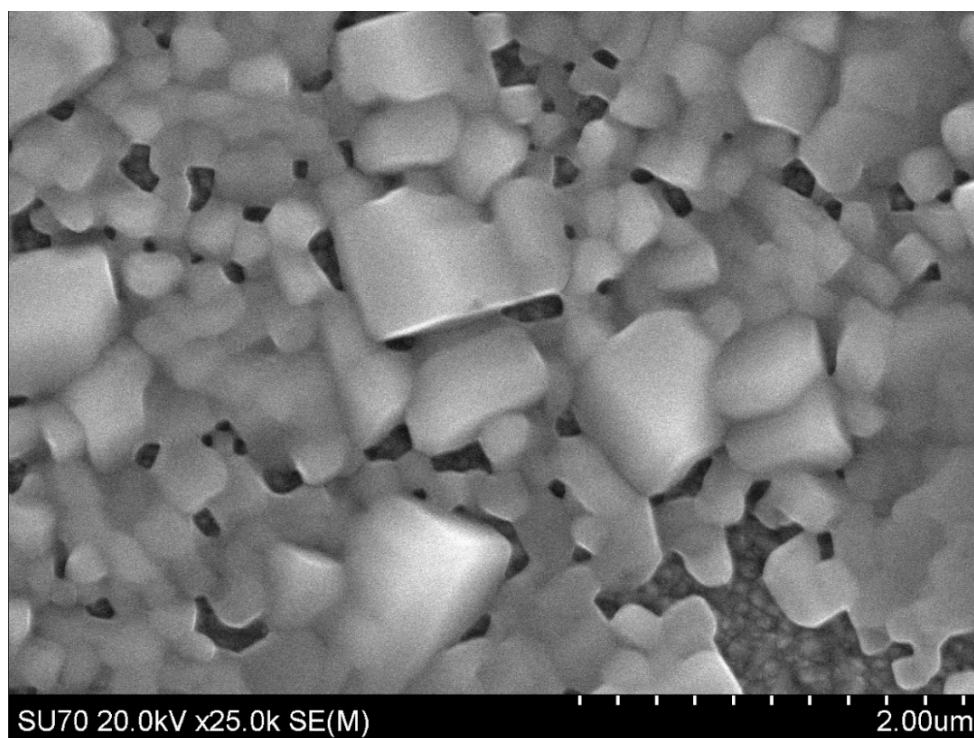


Figure 14. SEM of Perovskite Layer with Poly(TFEMA) Deposition

Scanning Electron Microscope (SEM) measurements were performed to characterize the Perovskite film surface morphology before and after deposition of Poly(TFEMA). Figure 11 shows the morphology of a film without any deposit and results in bumpy small grains. Figure 12 shows the morphology of a film with the fluoropolymer deposit in the supercritical CO₂ pressure vessel and results in a layer of large crystalline grains on top of bumpy small grains shown in figure 11. It can be assumed that the large grains layered on top of the small grains is the deposited poly(TFEMA).

4. Conclusion

In summary, the cloud point determination of Poly(TFEMA) in the solution of supercritical CO₂ and Ethanol was determined to achieve a deposition of the fluoropolymer on perovskite thin

films. This deposit can be used to enhance the perovskite film's hydrophobic properties.

However this study does not take into account the quality of the fluoropolymer film deposition. It should be possible to tune this method to be able to produce a deposition film with improved grain structure. This method can also be used on a wide range of thin films that experience high degradation rates from moisture.

References

1. Best research-cell efficiency chart. NREL.gov.
<https://www.nrel.gov/pv/cell-efficiency.html>
2. Lee, M. M., Teuscher, J., Miyasaka, T., Murakami, T. N., & Snaith, H. J. (2012). Efficient hybrid solar cells based on meso-superstructured organometal halide perovskites. *Science*, 338(6107), 643-647.
3. Miyata, A., Mitiglu, A., Plochocka, P., Portugall, O., Wang, J. T. W., Stranks, S. D., ... & Nicholas, R. J. (2015). Direct measurement of the exciton binding energy and effective masses for charge carriers in organic–inorganic tri-halide perovskites. *Nature Physics*, 11(7), 582-587
4. Eperon, G. E., Stranks, S. D., Menelaou, C., Johnston, M. B., Herz, L. M., & Snaith, H. J. (2014). Formamidinium lead trihalide: a broadly tunable perovskite for efficient planar heterojunction solar cells. *Energy & Environmental Science*, 7(3), 982-988.
5. Yang, W. S., Noh, J. H., Jeon, N. J., Kim, Y. C., Ryu, S., Seo, J., & Seok, S. I. (2015). High-performance photovoltaic perovskite layers fabricated through intramolecular exchange. *Science*, 348(6240), 1234-1237.
6. Stranks, S. D., Eperon, G. E., Grancini, G., Menelaou, C., Alcocer, M. J., Leijtens, T., ... & Snaith, H. J. (2013). Electron-hole diffusion lengths exceeding 1 micrometer in an organometal trihalide perovskite absorber. *Science*, 342(6156), 341-344.
7. Steirer, K. X., Schulz, P., Teeter, G., Stevanovic, V., Yang, M., Zhu, K., & Berry, J. J. (2016). Defect tolerance in methylammonium lead triiodide perovskite. *ACS Energy Letters*, 1(2), 360-366.
8. Annohene, G., & Tepper, G. C. (2021). Efficient perovskite solar cells processed in supercritical carbon dioxide. *The Journal of Supercritical Fluids*, 171, 105203.
9. Dhoble, S. J. (2021). Chapter 9.2 - Perovskite solar cells. In *Energy Materials: Fundamentals to applications*. essay, Elsevier.
10. Gao, Zhao, Y., Zhang, X., & You, J. (2020). Recent Progresses on Defect Passivation toward Efficient Perovskite Solar Cells. *Advanced Energy Materials.*, 10(13).
<https://doi.org/10.1002/aenm.201902650>
11. S. Sun, T. Salim, N. Mathews et al., “The origin of high efficiency in low-temperature solution-processable bilayer organometal halide hybrid solar cells,” *Energy Environ. Sci.*, vol. 7, no. 1, pp. 399–407, 2014
12. Perovskite Solar Cells. NREL.gov. (n.d.).
<https://www.nrel.gov/pv/perovskite-solar-cells.html>
13. Zhou, D., Zhou, T., Tian, Y., Zhu, X., & Tu, Y. (2018). Perovskite-Based Solar Cells: Materials, Methods, and Future Perspectives. *Journal of Nanomaterials*, 2018, 1-15.
14. Huang, F., Li, M., Šiffalovič, P., Cao, G., & Tian, J. (2019). From scalable solution fabrication of perovskite films towards commercialization of solar cells. *Energy & Environmental Science*.

15. Large-scale deposition of organic solar cells. Ossila. (n.d.).
<https://www.ossila.com/en-us/pages/opv-large-scale-deposition>
16. Nie. (2015). High-efficiency solution-processed perovskite solar cells with millimeter-scale grains. *Science.*, 347(6221), 522–525.
<https://doi.org/10.1126/science.aaa0472>
17. Sanli, D., Bozbag, S. E., & Erkey, C. (2012). Synthesis of nanostructured materials using supercritical CO₂: Part I. Physical transformations. *Journal of Materials Science*, 47(7), 2995-3025.
18. Libretexts. (2023, February 26). 12.4: Phase diagrams. Chemistry LibreTexts.
https://chem.libretexts.org/Bookshelves/General_Chemistry/Map%3A_General_Chemistry_%28Petrucci_et_al.%29/12%3A_Intermolecular_Forces%3A_Liquids_And_Solids/12.4%3A_Phase_Diagrams
19. Nie. (2015). High-efficiency solution-processed perovskite solar cells with millimeter-scale grains. *Science.*, 347(6221), 522–525.
<https://doi.org/10.1126/science.aaa0472>
20. Annohene, G., Pascucci, J., Pestov, D., & Tepper, G. C. (2020). Supercritical fluid-assisted crystallization of CH₃NH₃PbI₃ perovskite films. *The Journal of Supercritical Fluids*, 156, 104684.
21. Wu, W., Ke, J., & Poliakoff, M. (2006). Phase boundaries of CO₂+ toluene, CO₂+ acetone, and CO₂+ ethanol at high temperatures and high pressures. *Journal of Chemical & Engineering Data*, 51(4), 1398-1403.
22. Kwon, S., Bae, W., Lee, K., Byun, H. S., & Kim, H. (2007). High pressure phase behavior of carbon dioxide+ 2, 2, 2-trifluoroethyl methacrylate and+ poly (2, 2, 2-trifluoroethyl methacrylate) systems. *Journal of Chemical & Engineering Data*, 52(1), 89-92.
23. Ciardelli, F., Aglietto, M., Di Mirabello, L. M., Passaglia, E., Giancristoforo, S., Castelvetro, V., & Ruggeri, G. (1997). New fluorinated acrylic polymers for improving weatherability of building stone materials. *Progress in organic coatings*, 32(1-4), 43-50
24. Kwon, S., Bae, W., & Kim, H. (2004). The effect of CO₂ in free-radical polymerization of 2, 2, 2-trifluoroethyl methacrylate. *Korean Journal of Chemical Engineering*, 21, 910-914.
25. Ratcharak, O., & Sane, A. (2014). Surface coating with poly (trifluoroethyl methacrylate) through rapid expansion of supercritical CO₂ solutions. *The Journal of Supercritical Fluids*, 89, 106-112.
26. Lambermont-Thijs, H. M., Van Kuringen, H. P., van der Put, J. P., Schubert, U. S., & Hoogenboom, R. (2010). Temperature induced solubility transitions of various poly (2-oxazoline) s in ethanol-water solvent mixtures. *Polymers*, 2(3), 188-199.